Magnetic dynamo in galaxies and the origin of the far-infrared–radio correlation

Christoph Pfrommer[1]

in collaboration with

M. Werhahn[1], R. Pakmor[2], P. Girichidis[3], C. Simpson[4]
[1]AIP Potsdam, [2]MPA Garching, [3]U of Heidelberg, [4]U of Chicago

Cosmic Interacting Matters Workshop: cosmic ray transport and magnetic fields in the ISM and the CGM, Bochum, Oct 2022

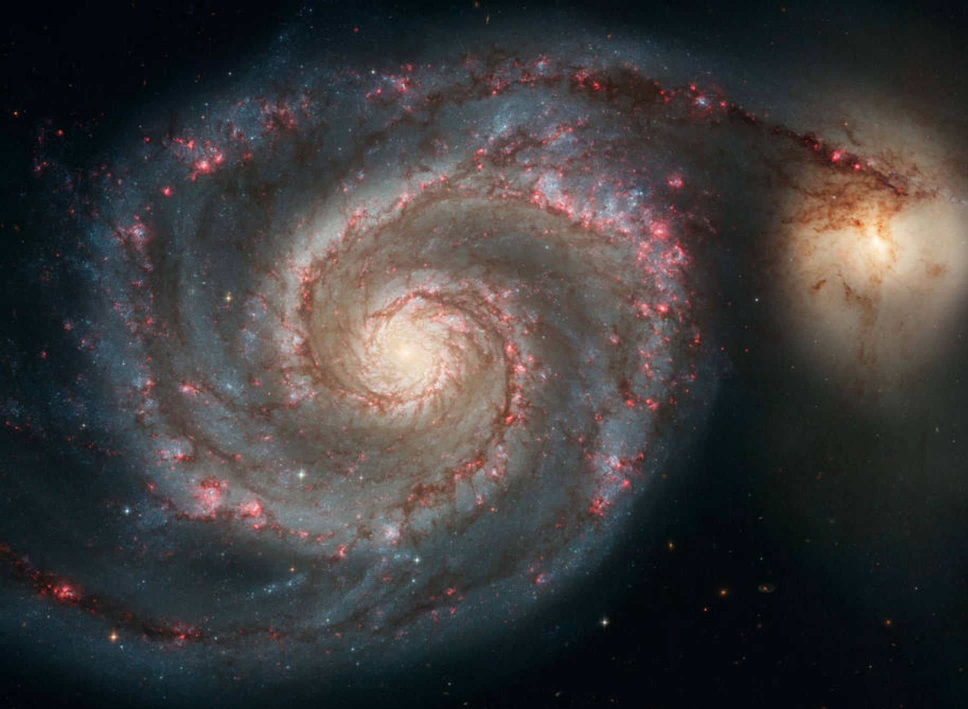

Outline

AIP

Origin and growth of magnetic fields

The general picture:

- ***Origin.*** Magnetic fields are generated by 1. electric currents sourced by a phase transition in the early universe or 2. by the Biermann battery

Origin and growth of magnetic fields

The general picture:

- ***Origin.*** Magnetic fields are generated by 1. electric currents sourced by a phase transition in the early universe or 2. by the Biermann battery
- ***Growth.*** A small-scale (fluctuating) dynamo is an MHD process, in which the kinetic (turbulent) energy is converted into magnetic energy: the mechanism relies on magnetic fields to become stronger when the field lines are stretched

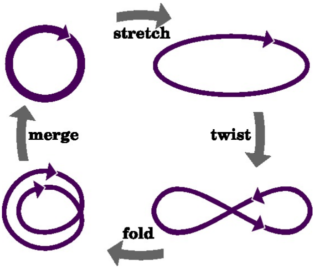

Origin and growth of magnetic fields

The general picture:

- ***Origin.*** Magnetic fields are generated by 1. electric currents sourced by a phase transition in the early universe or 2. by the Biermann battery
- ***Growth.*** A small-scale (fluctuating) dynamo is an MHD process, in which the kinetic (turbulent) energy is converted into magnetic energy: the mechanism relies on magnetic fields to become stronger when the field lines are stretched
- ***Saturation.*** Field growth stops at a sizeable fraction of the turbulent energy when magnetic forces become strong enough to resist the stretching and folding motions

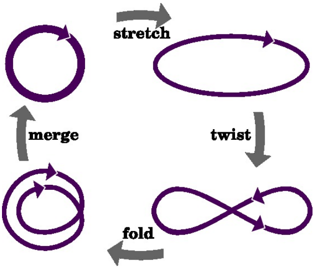

AIP

MHD-CR galaxy simulations

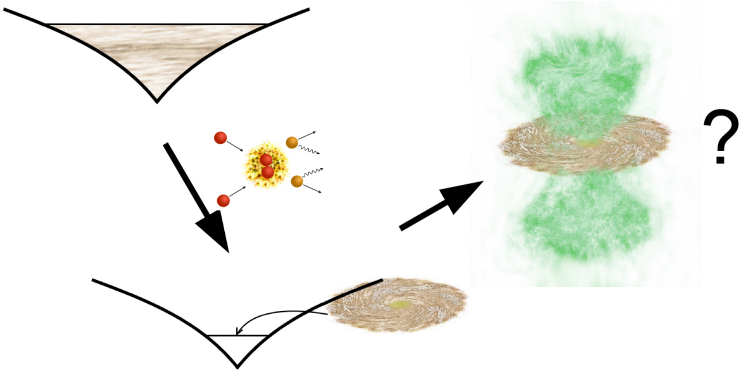

CP, Werhahn, Pakmor, Girichidis, Simpson (2022)
Simulating radio synchrotron emission in star-forming galaxies: small-scale magnetic dynamo and the origin of the far-infrared–radio correlation

MHD + cosmic ray advection + diffusion: $\{10^{10}, 10^{11}, 3 \times 10^{11}, 10^{12}\}\ \mathrm{M}_{\odot}$

Time evolution of SFR and energy densities

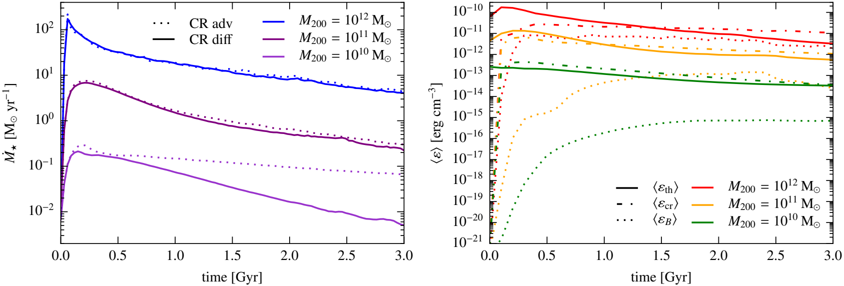

CP+ (2022)

- cosmic ray (CR) pressure feedback suppresses SFR more in smaller galaxies
- energy budget in disks is dominated by CR pressure
- magnetic growth faster in Milky Way galaxies than in dwarfs

Time evolution of CR and magnetic energy densities

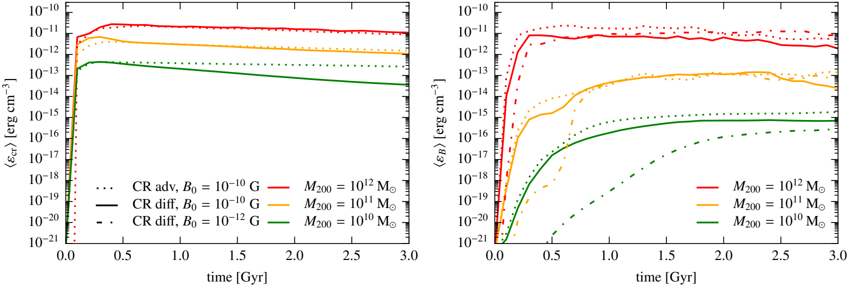

CP+ (2022)

- CRs diffuse out of galaxies $\Rightarrow$ lowers ε_{cr} in disk
- CR diffusion slows magnetic field growth $\Rightarrow$ lowers ε_B
- both effects decrease synchrotron emissivity
- magnetic field reaches saturation after initial growth phase

AIP

Time evolution of CR and magnetic energy densities

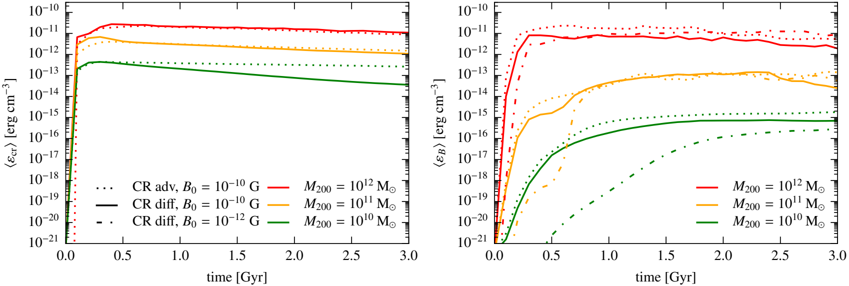

CP+ (2022)

- CRs diffuse out of galaxies $\Rightarrow$ lowers $\varepsilon_{\rm cr}$ in disk
- CR diffusion slows magnetic field growth $\Rightarrow$ lowers ε_B
- both effects decrease synchrotron emissivity
- magnetic field reaches saturation after initial growth phase
  $\Rightarrow$ study saturation stage!

Comparing turbulent and magnetic energy densities

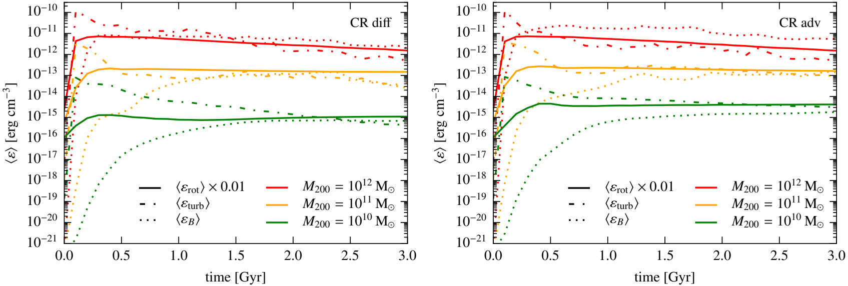

CP+ (2022)

- magnetic energy saturates at the turbulent energy, $\varepsilon_B \sim \varepsilon_{\rm turb} = \rho \delta v^2/2$ (averaged over the disk)
- saturation level similar for CR models with diffusion (left) and without (right)
- rotation dominates: $\varepsilon_{\rm rot} = \rho v_\varphi^2/2 \sim 100 \varepsilon_{\rm turb}$

Identifying different growth phases

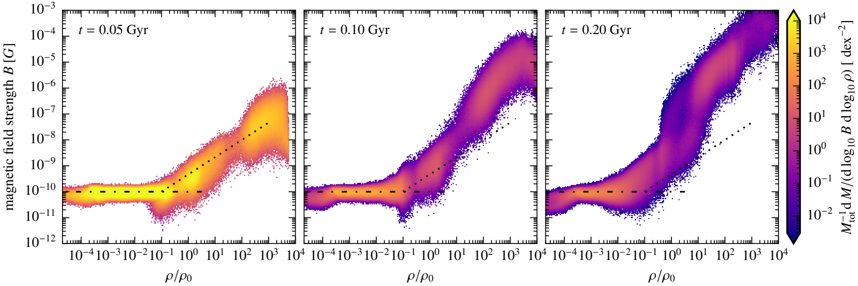

CP+ (2022)

- *1st phase:* adiabatic growth with $B \propto \rho^{2/3}$ (isotropic collapse)

Identifying different growth phases

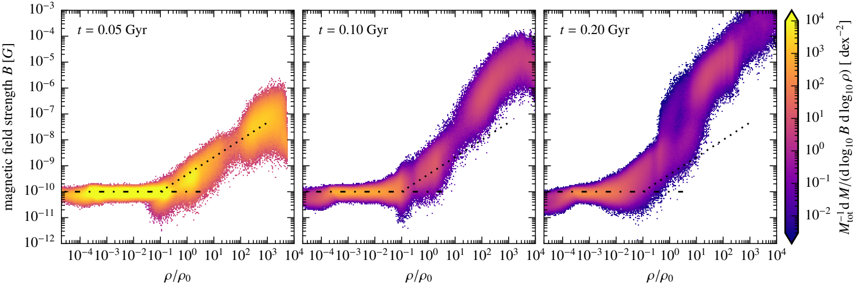

CP+ (2022)

- *1st phase:* adiabatic growth with $B \propto \rho^{2/3}$ (isotropic collapse)
- *2nd phase:* additional growth at high density ρ with small dynamical times $t_{\rm dyn} \sim (G\rho)^{-1/2}$

Identifying different growth phases

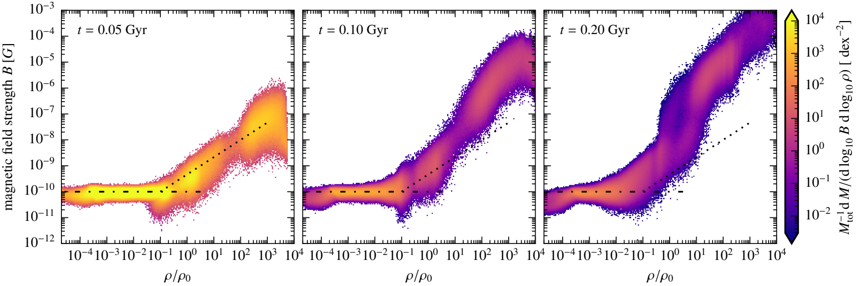

CP+ (2022)

- *1st phase:* adiabatic growth with $B \propto \rho^{2/3}$ (isotropic collapse)
- *2nd phase:* additional growth at high density ρ with small dynamical times $t_{\mathrm{dyn}} \sim (G\rho)^{-1/2}$
- *3rd phase:* growth migrates to lower ρ on larger scales $\propto \rho^{-1/3}$

Studying growth rate with numerical resolution

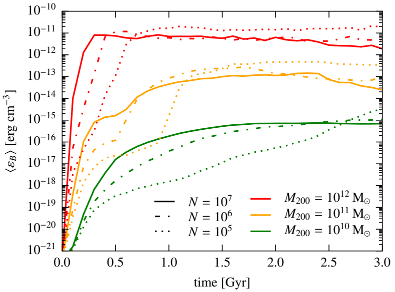

CP+ (2022)

- ***faster magnetic growth in higher resolution simulations and larger halos,*** numerical convergence for $N \gtrsim 10^6$

Studying growth rate with numerical resolution

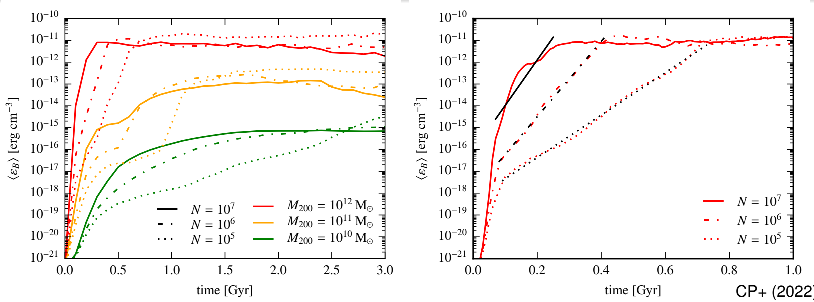

CP+ (2022)

- ***faster magnetic growth in higher resolution simulations and larger halos,*** numerical convergence for $N \gtrsim 10^6$
- *1st phase:* adiabatic growth (independent of resolution)

Studying growth rate with numerical resolution

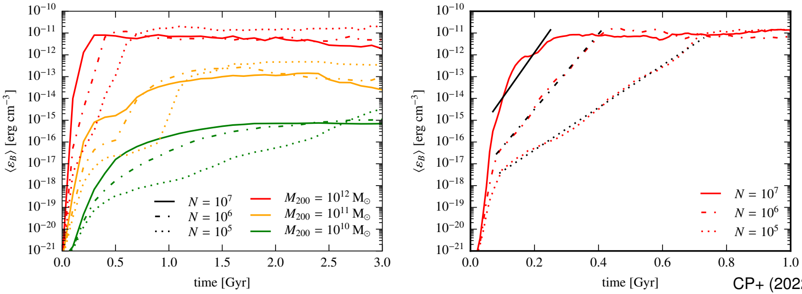

CP+ (2022)

- ***faster magnetic growth in higher resolution simulations and larger halos,*** numerical convergence for $N \gtrsim 10^6$
- *1st phase:* adiabatic growth (independent of resolution)
- *2nd phase:* small-scale dynamo with resolution-dep. growth rate

$$\Gamma = \frac{\mathcal{V}}{\mathcal{L}} \mathrm{Re}_{\mathrm{num}}^{1/2}, \quad \mathrm{Re}_{\mathrm{num}} = \frac{\mathcal{L}\mathcal{V}}{\nu_{\mathrm{num}}} = \frac{3\mathcal{L}\mathcal{V}}{d_{\mathrm{cell}}\, v_{\mathrm{th}}}$$

Exponential field growth in kinematic regime

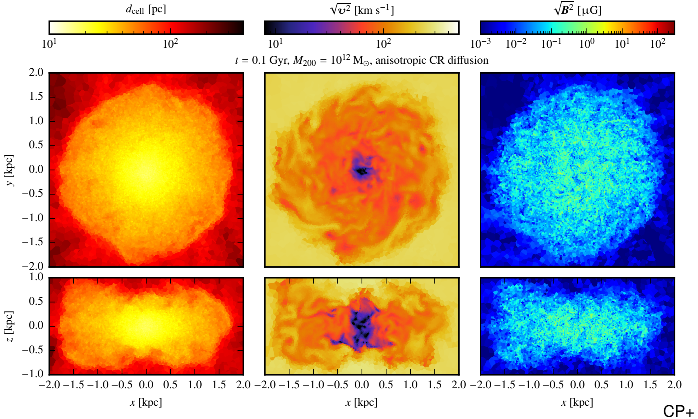

CP+ (2022)

- ***corrugated accretion shock*** dissipates kinetic energy from gravitational infall, injects vorticity that decays into turbulence, and drives a small-scale dynamo

Dynamo saturation on small scales while λ_B increases

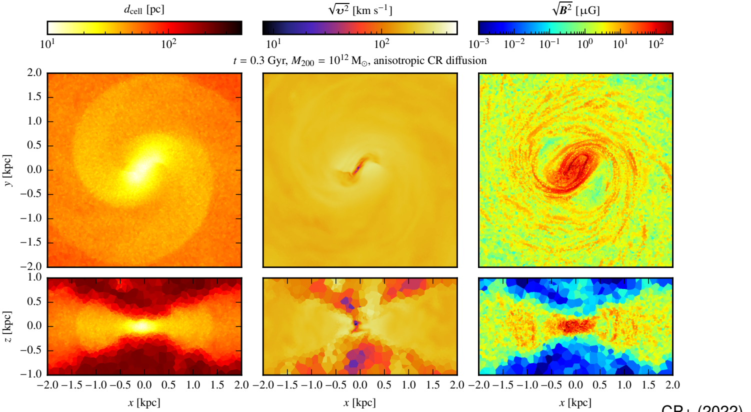

CP+ (2022)

- ***supersonic velocity shear*** between the rotationally supported cool disk and hotter CGM: excitation of Kelvin-Helmholtz body modes that interact and drive a small-scale dynamo

Kinetic and magnetic power spectra

Fluctuating small-scale dynamo in different analysis regions

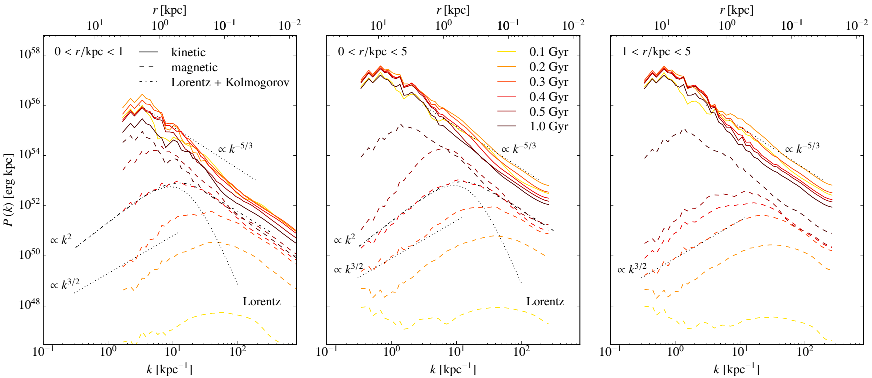

CP+ (2022)

- $E_B(k)$ superposition of form factor and turbulent spectrum
- pure turbulent spectrum outside steep central B profile

Kinetic and magnetic power spectra: different halos

Saturation mechanisms of fluctuating small-scale dynamo

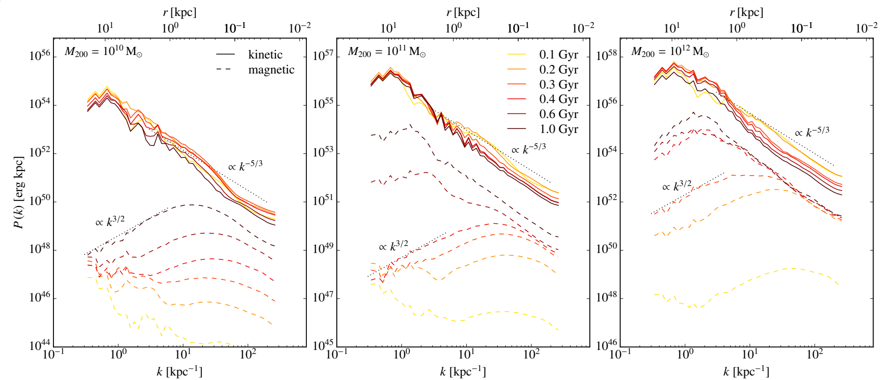

CP+ (2022)

- λ_B growth saturates close to equipartition in Milky Way
- λ_B growth stalls in dwarf galaxies: no equipartition with $\varepsilon_{\mathrm{th}}$

Non-thermal emission in star-forming galaxies

- ***previous theoretical modeling:***
  - one-zone steady-state models
    (Lacki+ 2010, 2011, Yoast-Hull+ 2013)
  - 1D transport models (Heesen+ 2016)
  - static Milky Way models
    (Strong & Moskalenko 1998, Evoli+ 2008, Kissmann 2014)

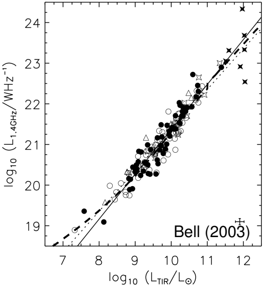

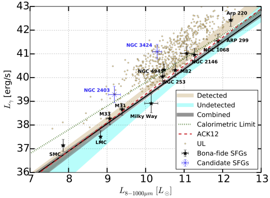

Ajello+ (2020)

Non-thermal emission in star-forming galaxies

- ***previous theoretical modeling:***
  - one-zone steady-state models (Lacki+ 2010, 2011, Yoast-Hull+ 2013)
  - 1D transport models (Heesen+ 2016)
  - static Milky Way models (Strong & Moskalenko 1998, Evoli+ 2008, Kissmann 2014)
- ***our theoretical modeling:***
  - run MHD-CR simulations of galaxies at different halos masses and SFRs
  - model steady-state CRs: protons, primary and secondary electrons
  - model all radiative processes from radio to gamma rays
  - gamma rays: understand pion decay and leptonic inverse Compton emission
  - radio: understand magnetic dynamo, primary and secondary electrons

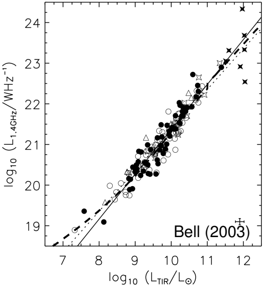

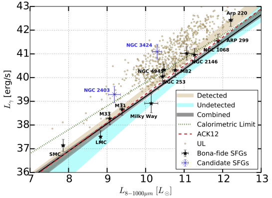

Ajello+ (2020)

Steady-state cosmic ray spectra

- solve the steady-state equation in every cell for each CR population:

$$\frac{N(E)}{\tau_{\mathrm{esc}}} - \frac{\mathrm{d}}{\mathrm{d}E}\left[N(E)b(E)\right] = Q(E)$$

- protons: Coulomb, hadronic and escape losses (re-normalized to $\varepsilon_{\mathrm{cr}}$)
- electrons: Coulomb, bremsstr., IC, synchrotron and escape losses
  - primaries (re-normalized using $K_{\mathrm{ep}} = 0.02$)
  - secondaries

Steady-state cosmic ray spectra

- solve the steady-state equation in every cell for each CR population:

$$\frac{N(E)}{\tau_\mathrm{esc}} - \frac{\mathrm{d}}{\mathrm{d}E}\left[N(E)b(E)\right] = Q(E)$$

- protons: Coulomb, hadronic and escape losses (re-normalized to ε_cr)
- electrons: Coulomb, bremsstr., IC, synchrotron and escape losses
  - primaries (re-normalized using $K_\mathrm{ep} = 0.02$)
  - secondaries
- steady state assumption is fulfilled in disk and in regions dominating the non-thermal emission but not at low densities, at SNRs and in outflows

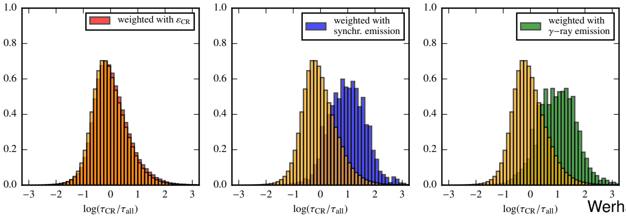

Werhahn+ (2021a)

Simulated radio emission: $10^{12}\,\mathrm{M}_\odot$ halo

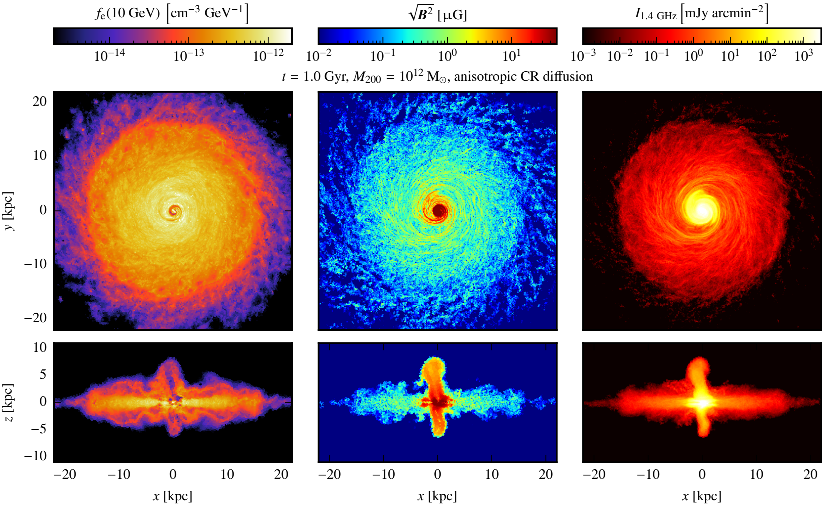

CP+ (2022)

Simulated radio emission: 10^{11} $M_\odot$ halo

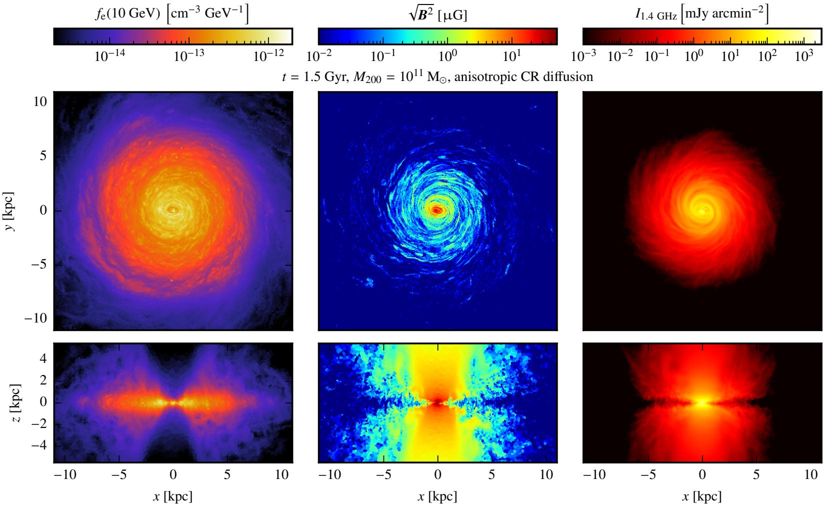

CP+ (2022)

Far infra-red – radio correlation

Universal conversion: star formation → cosmic rays → radio

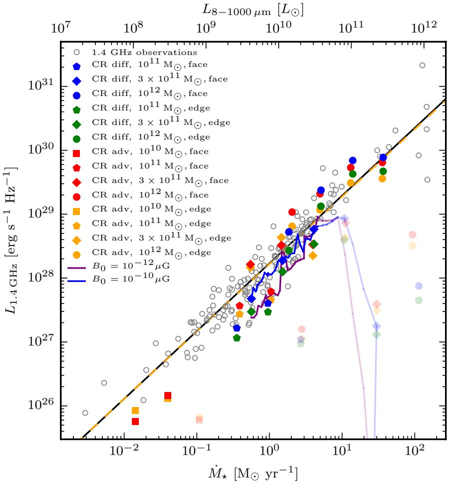

CP+ (2022)

Simulated radio emission: $10^{12}\,\mathrm{M}_\odot$ halo

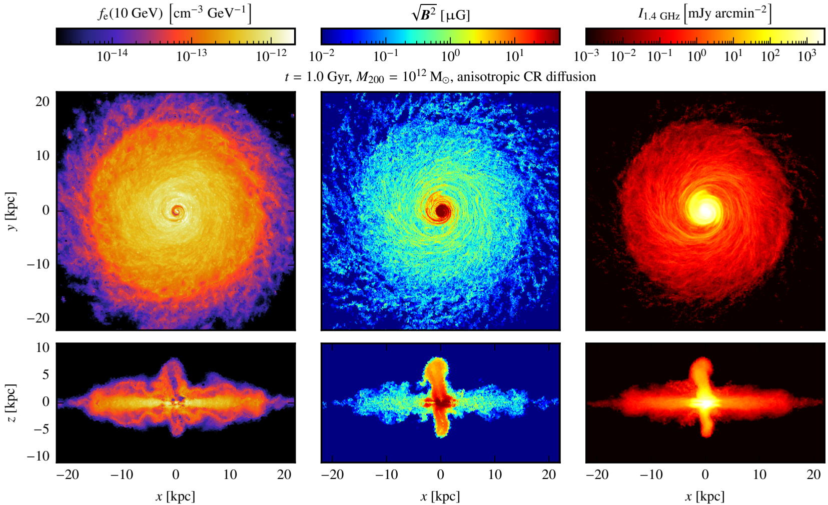

CP+ (2022)

Local FIR-to-radio correlation, $10^{12}\,\mathrm{M}_\odot$ halo

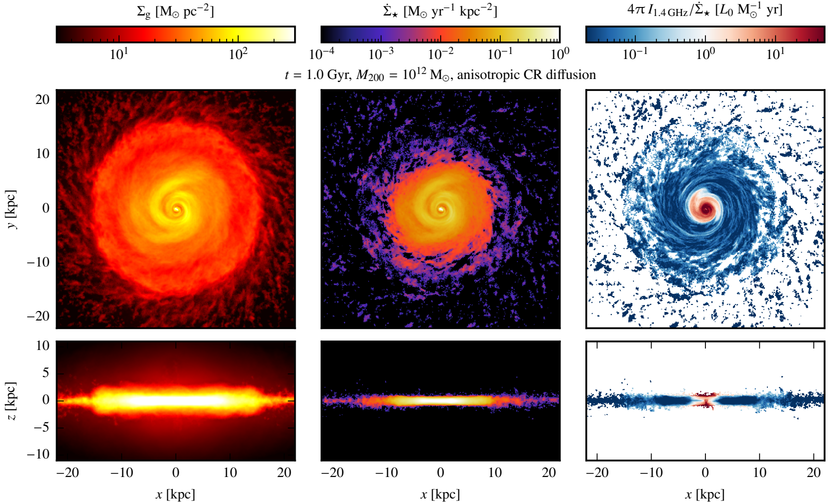

CP+ (2022)

Local FIR-to-radio correlation, 10^{11} M$_\odot$ halo

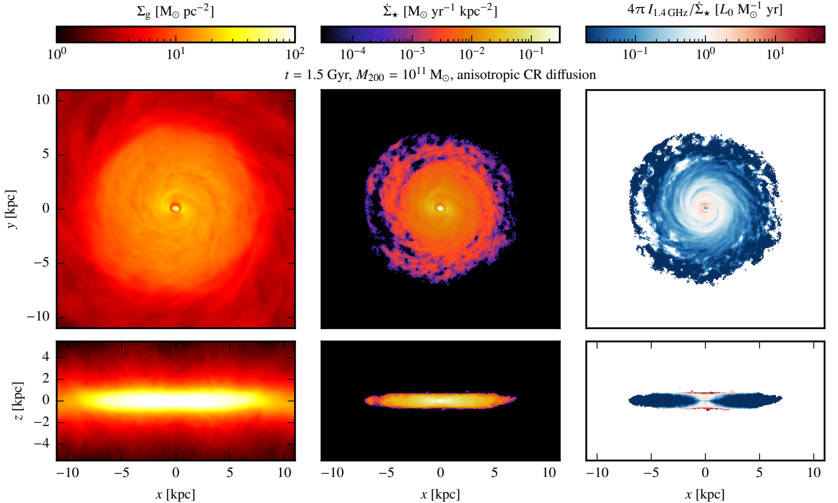

CP+ (2022)

Conclusions

- energy budget in large galaxies is dominated by CR pressure $\Rightarrow$ star formation suppressed
- fluctuating small-scale dynamo grows magnetic fields in isolated galaxies: driven by (i) corrugated accretion shock and (ii) Kelvin-Helmholtz body modes excited by disk-halo velocity shear
- small-scale dynamo clearly identified via growth rates, saturation at $\varepsilon_B \sim \varepsilon_{\mathrm{turb}}$, power spectra, magnetic curvature statistics

Conclusions

- energy budget in large galaxies is dominated by CR pressure
  $\Rightarrow$ star formation suppressed
- fluctuating small-scale dynamo grows magnetic fields in isolated galaxies: driven by (i) corrugated accretion shock and (ii) Kelvin-Helmholtz body modes excited by disk-halo velocity shear
- small-scale dynamo clearly identified via growth rates, saturation at $\varepsilon_B \sim \varepsilon_{\mathrm{turb}}$, power spectra, magnetic curvature statistics
- magnetic fields saturate close to equipartition in Milky Way centers and sub-equipartition at larger radii and in dwarfs
  $\Rightarrow$ issue with ISM modeling and missing large-scale dynamo?
- global $L_{\mathrm{FIR}} - L_{\mathrm{radio}}$ reproduced for galaxies with saturated magnetic fields, scatter due to viewing angle and CR transport
- local $L_{\mathrm{FIR}} - L_{\mathrm{radio}}$ reproduced at larger radii, but not in centers

PICOGAL: From Plasma KInetics to COsmological GALaxy Formation

This project has received funding from the European Research Counsil (ERC) under the European Union's Horizon 2020 research and innovation program (grant agreement No PICOGAL–101019746).

Additional slides

Lorentz force: magnetic curvature and pressure

- Lorentz force density, expressed in terms of $\boldsymbol{B}$ in the MHD approximation:

$$\boldsymbol{f}_{\mathrm{L}} = \frac{1}{c}\boldsymbol{j}\times\boldsymbol{B} = \frac{1}{4\pi}(\nabla\times\boldsymbol{B})\times\boldsymbol{B} = \frac{1}{4\pi}(\boldsymbol{B}\cdot\nabla)\,\boldsymbol{B} - \frac{1}{8\pi}\nabla B^2,$$

two terms on RHS are ***not*** magnetic curvature and pressure forces!

Lorentz force: magnetic curvature and pressure

- Lorentz force density, expressed in terms of $\boldsymbol{B}$ in the MHD approximation:

$$\boldsymbol{f}_\mathrm{L} = \frac{1}{c}\boldsymbol{j}\times\boldsymbol{B} = \frac{1}{4\pi}\left(\boldsymbol{\nabla}\times\boldsymbol{B}\right)\times\boldsymbol{B} = \frac{1}{4\pi}\left(\boldsymbol{B}\cdot\boldsymbol{\nabla}\right)\boldsymbol{B} - \frac{1}{8\pi}\boldsymbol{\nabla}B^2,$$

two terms on RHS are ***not*** magnetic curvature and pressure forces!

- define $\boldsymbol{B} = B\boldsymbol{b}$, where $\boldsymbol{b}$ is the unit vector along $\boldsymbol{b}$ and rewrite $\boldsymbol{f}_\mathrm{L}$:

$$\begin{aligned}\boldsymbol{f}_\mathrm{L} &= \frac{B^2}{4\pi}\left(\boldsymbol{b}\cdot\boldsymbol{\nabla}\right)\boldsymbol{b} + \frac{1}{8\pi}\boldsymbol{b}(\boldsymbol{b}\cdot\boldsymbol{\nabla})B^2 - \frac{1}{8\pi}\boldsymbol{\nabla}B^2\\ &= \frac{B^2}{4\pi}\left(\boldsymbol{b}\cdot\boldsymbol{\nabla}\right)\boldsymbol{b} - \frac{1}{8\pi}\boldsymbol{\nabla}_\perp B^2 \equiv \boldsymbol{f}_\mathrm{c} + \boldsymbol{f}_\mathrm{p},\end{aligned}$$

where $\boldsymbol{\nabla}_\perp = (\mathbf{1} - \boldsymbol{b}\boldsymbol{b})\cdot\boldsymbol{\nabla}$ is the perpendicular gradient

Lorentz force: magnetic curvature and pressure

- Lorentz force density, expressed in terms of $\boldsymbol{B}$ in the MHD approximation:
$$\boldsymbol{f}_\mathrm{L} = \frac{1}{c}\boldsymbol{j}\times\boldsymbol{B} = \frac{1}{4\pi}(\boldsymbol{\nabla}\times\boldsymbol{B})\times\boldsymbol{B} = \frac{1}{4\pi}(\boldsymbol{B}\cdot\boldsymbol{\nabla})\boldsymbol{B} - \frac{1}{8\pi}\boldsymbol{\nabla}B^2,$$
two terms on RHS are ***not*** magnetic curvature and pressure forces!
- define $\boldsymbol{B} = B\boldsymbol{b}$, where $\boldsymbol{b}$ is the unit vector along $\boldsymbol{b}$ and rewrite $\boldsymbol{f}_\mathrm{L}$:
$$\begin{aligned}\boldsymbol{f}_\mathrm{L} &= \frac{B^2}{4\pi}(\boldsymbol{b}\cdot\boldsymbol{\nabla})\boldsymbol{b} + \frac{1}{8\pi}\boldsymbol{b}(\boldsymbol{b}\cdot\boldsymbol{\nabla})B^2 - \frac{1}{8\pi}\boldsymbol{\nabla}B^2\\ &= \frac{B^2}{4\pi}(\boldsymbol{b}\cdot\boldsymbol{\nabla})\boldsymbol{b} - \frac{1}{8\pi}\boldsymbol{\nabla}_\perp B^2 \equiv \boldsymbol{f}_\mathrm{c} + \boldsymbol{f}_\mathrm{p},\end{aligned}$$
where $\boldsymbol{\nabla}_\perp = (\mathbf{1} - \boldsymbol{bb})\cdot\boldsymbol{\nabla}$ is the perpendicular gradient
$\Rightarrow$ $\boldsymbol{f}_\mathrm{c}$ is the magnetic curvature force and $\boldsymbol{f}_\mathrm{p}$ is $\perp$ mag. pressure force

Lorentz force: magnetic curvature and pressure

- Lorentz force density, expressed in terms of $\boldsymbol{B}$ in the MHD approximation:

$$\boldsymbol{f}_\mathrm{L} = \frac{1}{c}\boldsymbol{j}\times\boldsymbol{B} = \frac{1}{4\pi}(\nabla\times\boldsymbol{B})\times\boldsymbol{B} = \frac{1}{4\pi}(\boldsymbol{B}\cdot\nabla)\boldsymbol{B} - \frac{1}{8\pi}\nabla B^2,$$

  two terms on RHS are ***not*** magnetic curvature and pressure forces!
- define $\boldsymbol{B} = B\boldsymbol{b}$, where $\boldsymbol{b}$ is the unit vector along $\boldsymbol{b}$ and rewrite $\boldsymbol{f}_\mathrm{L}$:

$$\begin{aligned}\boldsymbol{f}_\mathrm{L} &= \frac{B^2}{4\pi}(\boldsymbol{b}\cdot\nabla)\boldsymbol{b} + \frac{1}{8\pi}\boldsymbol{b}(\boldsymbol{b}\cdot\nabla)B^2 - \frac{1}{8\pi}\nabla B^2 \\ &= \frac{B^2}{4\pi}(\boldsymbol{b}\cdot\nabla)\boldsymbol{b} - \frac{1}{8\pi}\nabla_\perp B^2 \equiv \boldsymbol{f}_\mathrm{c} + \boldsymbol{f}_\mathrm{p},\end{aligned}$$

  where $\nabla_\perp = (\mathbf{1} - \boldsymbol{bb})\cdot\nabla$ is the perpendicular gradient

  $\Rightarrow \boldsymbol{f}_\mathrm{c}$ is the magnetic curvature force and $\boldsymbol{f}_\mathrm{p}$ is $\perp$ mag. pressure force
- define a magnetic curvature:

$$\boldsymbol{\kappa} \equiv (\boldsymbol{b}\cdot\nabla)\boldsymbol{b} = \frac{(\mathbf{1} - \boldsymbol{bb})\cdot(\boldsymbol{B}\cdot\nabla)\boldsymbol{B}}{B^2} = \frac{4\pi\,\boldsymbol{f}_\mathrm{c}}{B^2},$$

Correlating magnetic curvature to field strength – 1

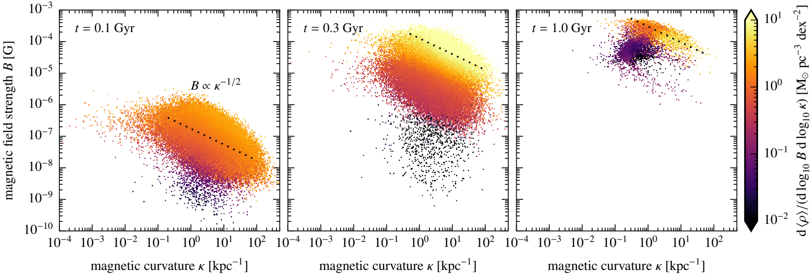

CP+ (2022)

- emergence of magnetic field and curvature in the galaxy centre
- panels show from left to right:

  (i) exponential growth phase in the kinematic regime
  (ii) growth of the magnetic coherence scale
  (iii) saturation phase of the magnetic dynamo

Correlating magnetic curvature to field strength – 2

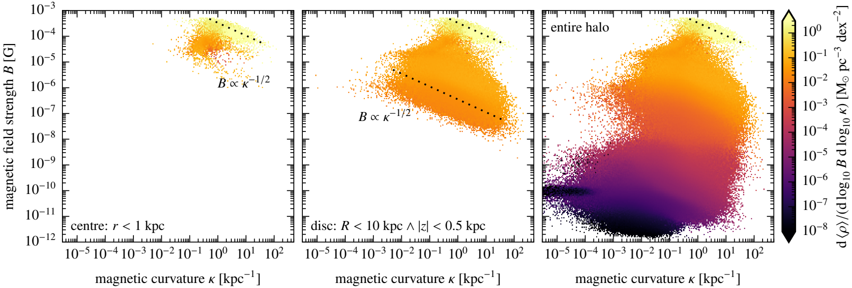

CP+ (2022)

- separating different dynamo processes by spatial cuts during saturated phase
- superposition of different small-scale dynamos
- each dynamo grows at a different characteristic density or eddy turnover time